Chile-Finnland Workshop on Biofuels

“Biotechnology for Biofuels”

Santiago, Chile (24-28 March 2008)
15 November 2010

BIOTECHNOLOGY 2004

12th international biotechnology symposium and exhibition

17-22 October 2004
Santiago, Chile
www.conicyt.cl/IBS2004


world congress
biotechnology
Sr. Sergio Bitar
Sr. Juan A.


BIOTECHNOLOGY
2004
12th international biotechnology
symposium and exhibition
17-22 October 2004
Santiago, Chile
BIOTECHNOLOGY
GOBIERNO DE CHILE
CONICYT
the world congress on biotechnology
2004


2004
the world congress on biotechnology

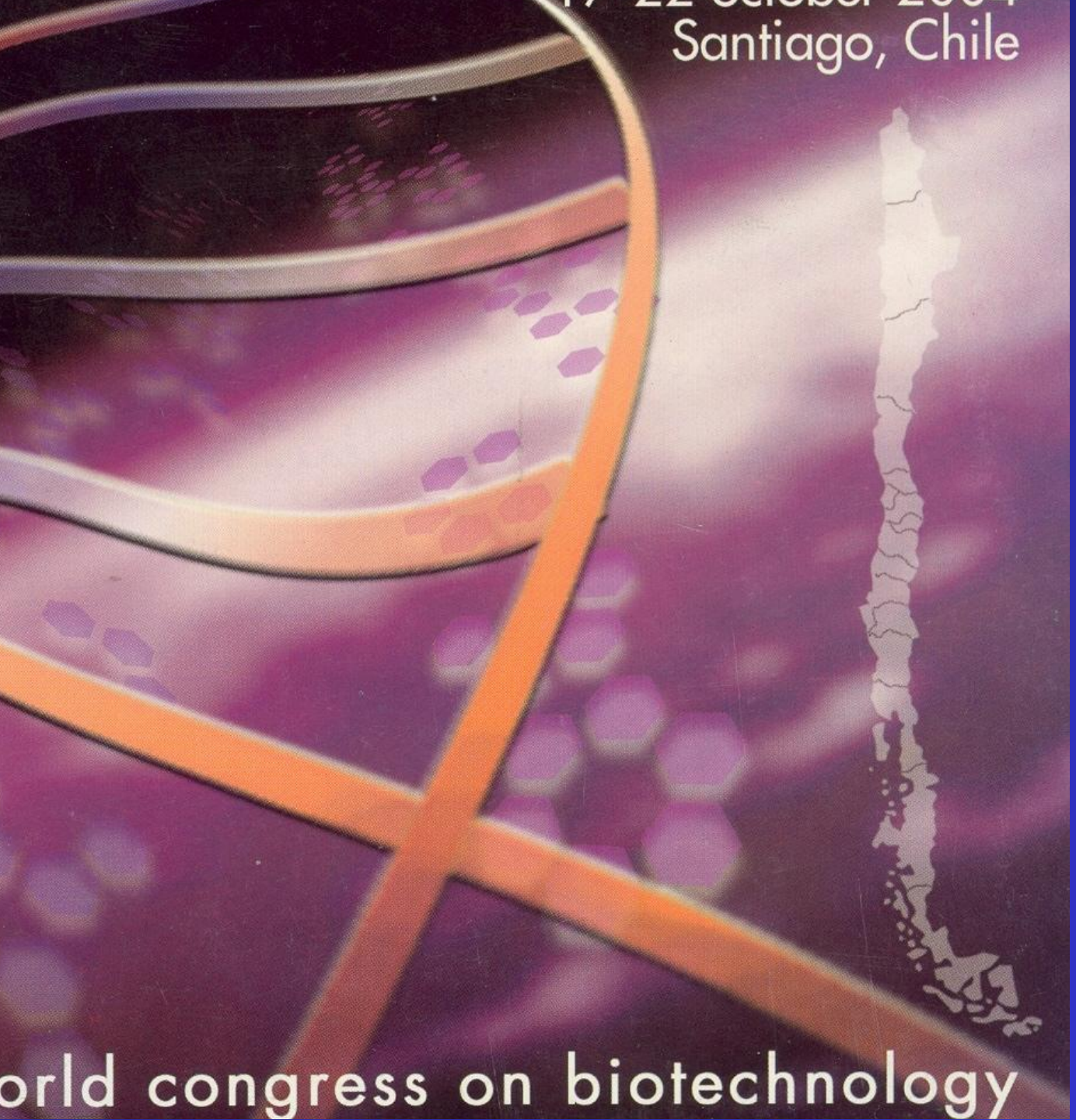
Santiago, Chile
orld congress on biotechnology

Santiago, Chile

ess on biotechnology

ARTICLE

BIOTECHNOLOGY and BIOENGINEERING

A Mechanistic Model of the Enzymatic Hydrolysis of Cellulose

Seth E. Levine, Jerome M. Fox, Harvey W. Blanch, Douglas S. Clark

Energy Biosciences Institute, Department of Chemical Engineering, University of California-Berkeley, Berkeley, California 94720; telephone: 510-642-2408; fax: 510-643-1228; e-mail: clark@berkeley.edu

Received 19 January 2010; revision received 16 April 2010; accepted 26 April 2010

Published online 18 May 2010 in Wiley InterScience (www.interscience.wiley.com). DOI 10.1002/bit.22789

BOX 1. Mapping Arbitrary Particle Shapes to Collections of Spheres

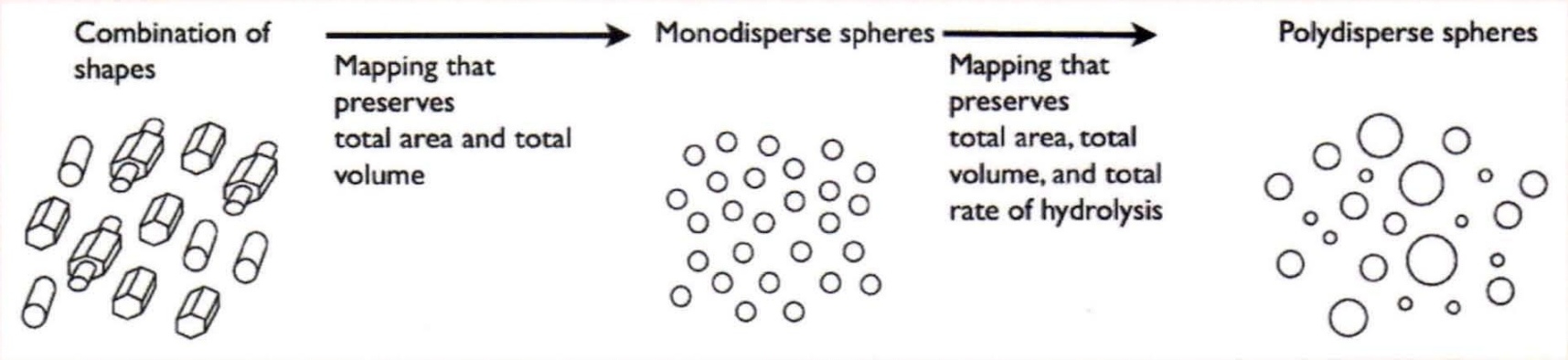

Monodisperse distributions of spheres can be used to model properties for static shapes. When the arbitrary shapes of interest change with time, a polydisperse distribution of spheres must be used to properly map the properties. Figure A1 shows the requirements and capabilities for matching static and dynamic properties of a given shape.

The polydisperse distribution of spheres required to map a given shape is difficult to determine. It requires knowledge of how the surface area changes with time. Thus a reverse approach may be used, where a given polydisperse distribution is used to model the dynamic change of a particle's properties. The form of these results is compared to measured results. Thus, instead of directly finding the sphere distribution to match an arbitrary shape, an arbitrary shape is found that matches a given sphere distribution.

Hydrolysis Mechanism

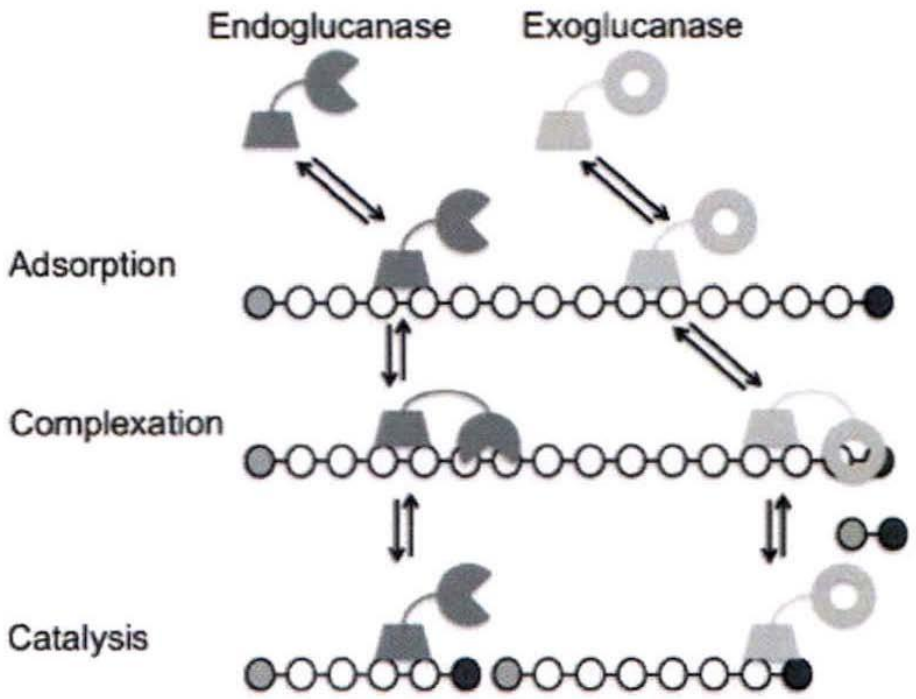

Figure 1. Schematic of the general mechanistic steps of cellulase-catalyzed hydrolysis of cellulose by an endoglucanase and an exoglucanase.

Table I. Kinetic parameters used in model simulations for comparison to experimental data from Medve et al. (1998).

Kinetic parameter	Value[a]	Units
$k_{EG2\text{-}ads}$	8640[b]	$L\,mmol^{-1}\,h^{-1}$
$k_{CBH1\text{-}ads}$	8640[b]	$L\,mmol^{-1}\,h^{-1}$
$k_{EG2\text{-}des}$	19.3[b]	hr^{-1}
$k_{CBH1\text{-}des}$	164[b]	hr^{-1}
$k_{cat\text{-}EG2}$	65[c]	s^{-1}
$k_{cat\text{-}CBH1}$	9.4[c]	s^{-1}
$K_{M\text{-}EG2\text{-}cel}$	0.0067[d]	$mmol\,dm^{-2}$
$K_{M\text{-}CBH1\text{-}cel}$	0.000014[d]	$mmol\,dm^{-2}$
$K_{M\text{-}EG2\text{-}sol}$	0.053[c]	$mmol\,L^{-1}$
$K_{M\text{-}CBH1\text{-}sol}$	0.0032[c]	$mmol\,L^{-1}$
$K_{i\text{-}EG2\text{-}cellobiose}$	0.01[d]	$mmol\,L^{-1}$
$K_{i\text{-}CBH1\text{-}cellobiose}$	0.093[d]	$mmol\,L^{-1}$
$K_{i\text{-}EG2\text{-}glucose}$	16.9[d]	$mmol\,L^{-1}$
$K_{i\text{-}CBH1\text{-}glucose}$	31[c]	$mmol\,L^{-1}$

[a]For expanded details about the model parameters and their sources see Appendix C in the Supplemental Material.

[b]Parameters based on values from elipsiometry experiments (unpublished data).

[c]Experimental parameters from various literature sources.

[d]Parameters optimized to early time data (less than 3 h) for single enzyme hydrolysis results from Medve et al. (1998).

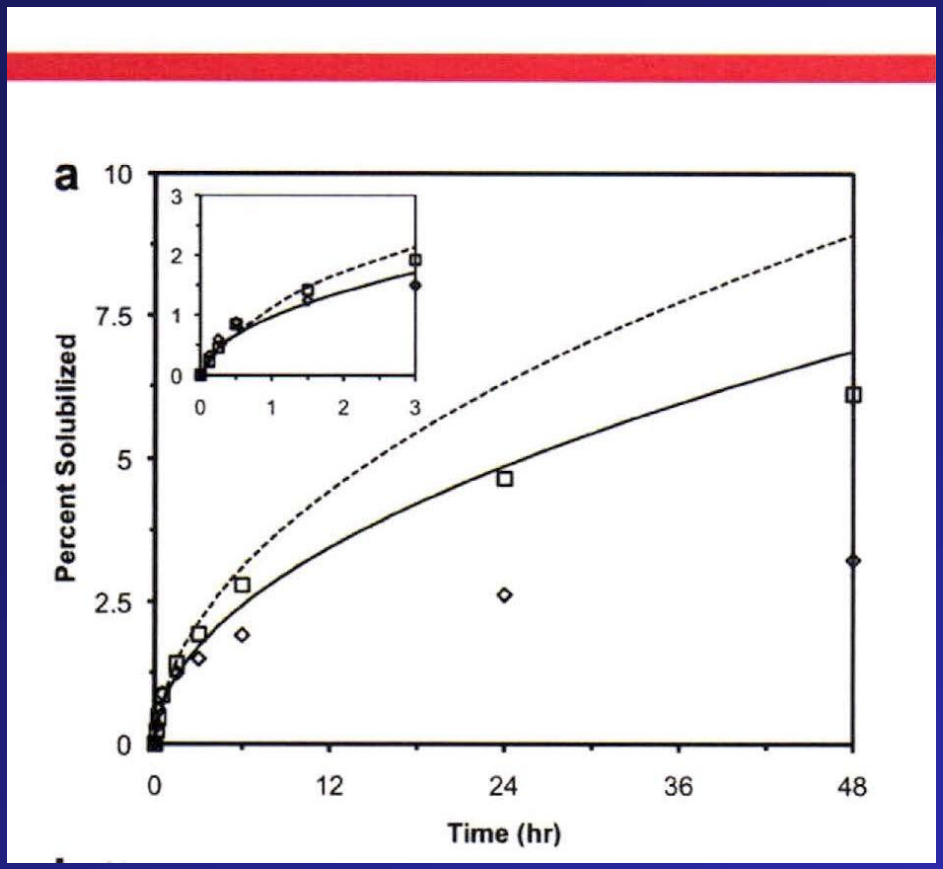

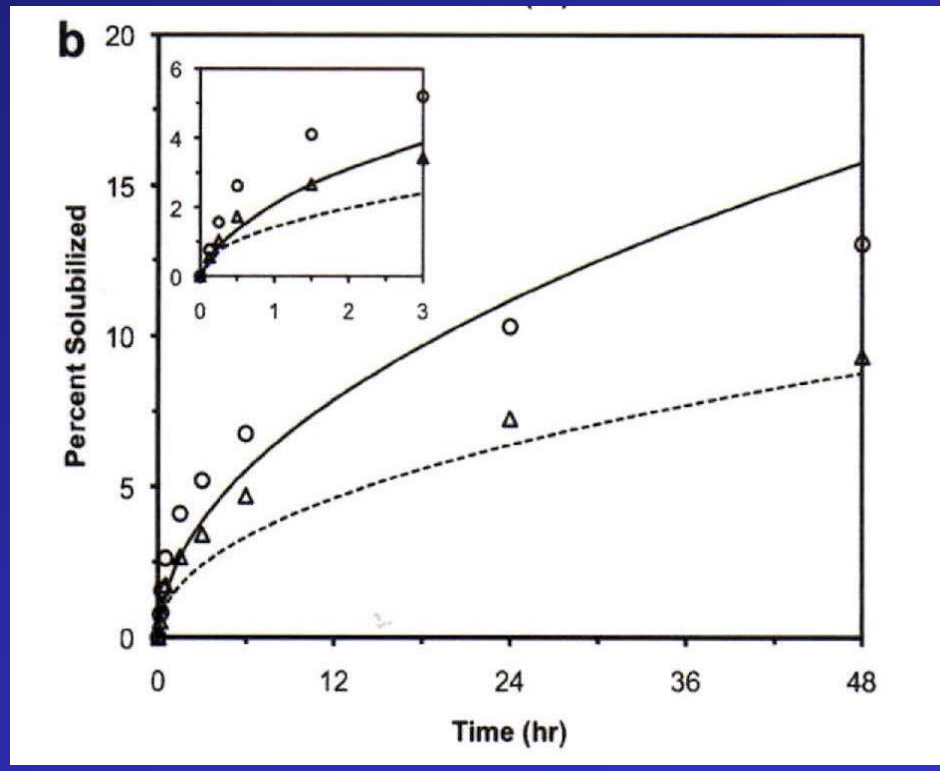

Figure 2. Model results using monodisperse spheres with the low initial surface area value ($8\,m^2\,g^{-1}$) compared to experimental data for (**a**) single enzyme hydrolysis with CBH1 (□, experiment; - - -, model) and EG2 (◇, experiment; —, model) and (**b**) theoretical mixed enzyme hydrolysis based on single enzyme experiments (△, experiment; —, model) and the actual mixture (○, experiment; - - -, model). The experimental data are from Medve et al. (1998). The insets show an expanded view of the early time points (up to 3 h).

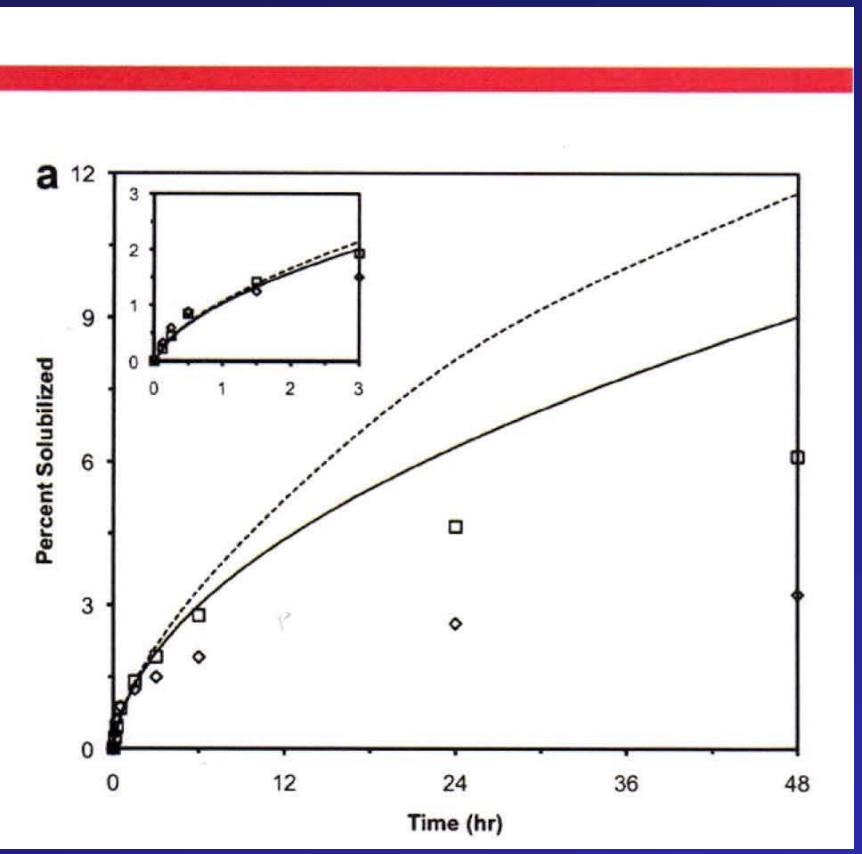

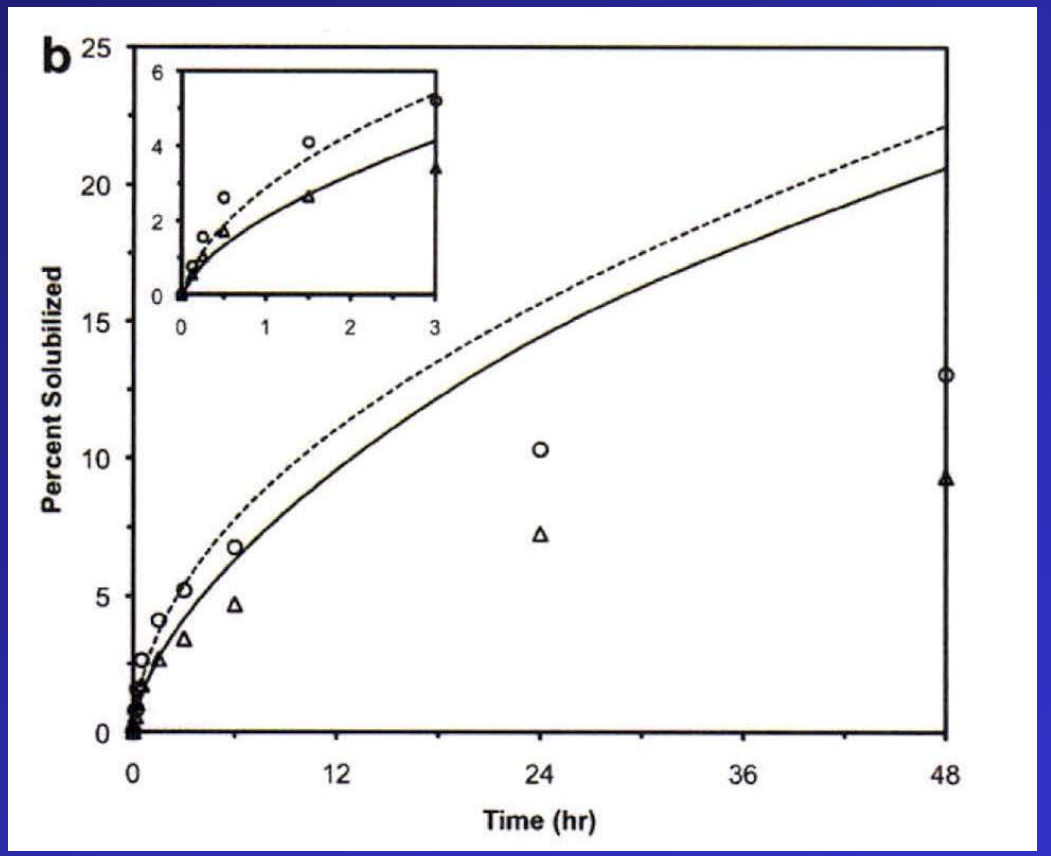

Figure 4. Model results using monodisperse spheres with the high initial surface area value (47.6 $m^2 g^{-1}$) compared to experimental data for (**a**) single enzyme hydrolysis with CBH1 (□, experiment; - - -, model) and EG2 (◇, experiment; —, model) and (**b**) theoretical mixed enzyme hydrolysis based on single enzyme experiments (△, experiment; —, model) and the actual mixture (○, experiment; - - -, model). The experimental data are from Medve et al. (1998). The insets show an expanded view of the early time points (up to 3 h).

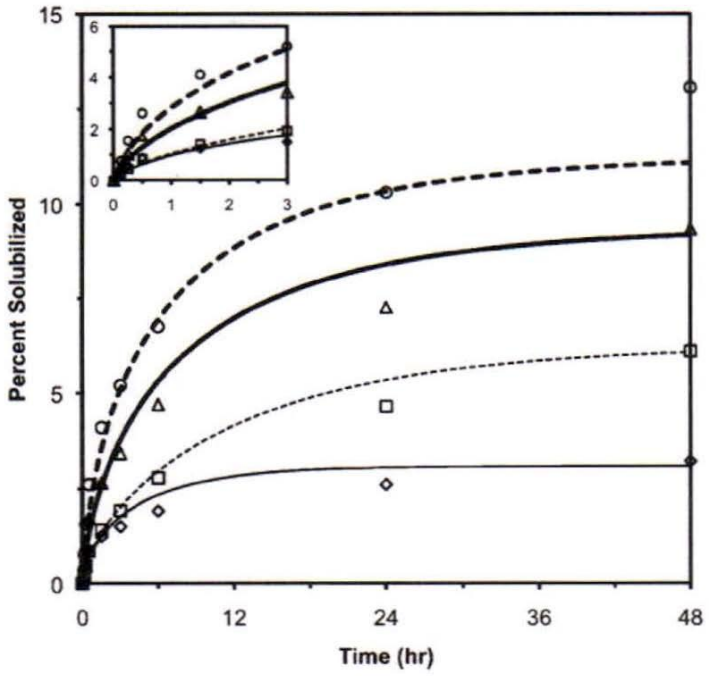

Figure 6. Comparison of model results with experimental data using monodisperse spheres with the high initial surface area (47.6 $m^2 g^{-1}$) case with the inclusion of first-order thermal enzyme deactivation in the model. Results are shown for hydrolysis with EG2 (◇, experiment; —, model), CBH1 (□, experiment; - - -, model), theoretical mixture from single enzyme hydrolysis results (△, experiment; **---**, model), and the actual EG2 and CBH1 mixture (○, experiment; **—**, model). The experimental data are from Medve et al. (1998). The insets show an expanded view of the early time points (up to 3 h).

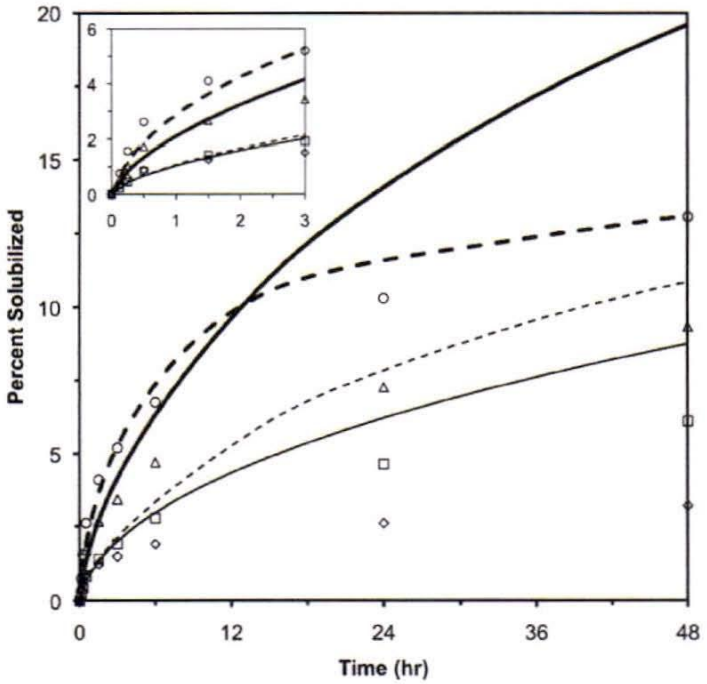

Figure 8. Comparison of model results with experimental data using a bimodal sphere distribution with 7.5 wt% 2.25 μm spheres and 92.5 wt% 139 μm spheres with an initial total surface area of 47.6 $m^2 g^{-1}$. Results are shown for hydrolysis with EG2 (◇, experiment; —, model), CBH1 (□, experiment; - - -, model), theoretical mixture from single enzyme hydrolysis results (△, experiment; **---**, model), and the actual EG2 and CBH1 mixture (○, experiment; **—**, model). The experimental data are from Medve et al. (1998). The insets show an expanded view of the early time points (up to 3 h).

Maximizing the Formation of Glucose in the Enzymatic Hydrolysis of Insoluble Cellulose

JUAN A. ASENJO

Biochemical Engineering Laboratory
Department of Chemical Engineering
and Applied Chemistry
Columbia University
New York, New York 10027

Accepted for Publication May 4, 1983

Biotechnology and Bioengineering, Vol. XXV, Pp. 3185–3190 (1983)

THEORY

A basic kinetic model with two rate-limiting steps can be used to model the hydrolysis of cellulose. The first step corresponds to the solubilization and depolymerization of the insoluble cellulose into cellobiose which includes adsorption of the soluble enzyme on the insoluble substrate. The second step is the hydrolysis of cellobiose into glucose. Both cellobiose and glucose inhibit the cellulase enzymes in the first step and glucose inhibits cellobiose hydrolysis in the second step. Substrate inhibition and temperature denaturation have been neglected. The reaction scheme is:

$$E \underset{k_{\text{des}}}{\overset{k_{\text{ads}}}{\rightleftharpoons}} E^* \tag{1}$$

$$E^* + S \rightleftharpoons E^*S \rightarrow E + Cb \tag{2}$$

Biotechnology and Bioengineering, Vol. XXV, Pp. 3185–3190 (1983)

$$E + Cb \rightleftharpoons ECb \tag{3}$$

$$E^* + Cb \rightleftharpoons E^*Cb \tag{3'}$$

$$E + G \rightleftharpoons EG \tag{4}$$

$$E^* + G \rightleftharpoons E^*G \tag{4'}$$

$$E_2 + Cb \rightleftharpoons E_2Cb \rightarrow E_2 + G \tag{5}$$

$$E_2 + G \rightleftharpoons E_2G \tag{6}$$

In the first reaction (eq. 1), the enzymes (E) adsorb on the insoluble cellulose, K_{ad} being the distribution coefficient of E between the solid and liquid phases:

$$\frac{E^*}{E} = \frac{k_{ads}}{k_{des}} = K_{ad} \tag{7}$$

and K_{ad} can be assumed to be constant at not too high enzyme concentrations ($E \leq 1$ g/L[7,8]). The adsorbed enzymes form the E^*S complex which irreversibly proceeds to yield cellobiose (Cb) and free enzyme (E) [eq. (2)]. Equations (3)–(4′) represent the competitive cellobiose and glucose inhibition effect on both the adsorbed and the soluble enzymes. Equations (5) and (6) show the cellobiose hydrolysis with competitive glucose inhibition. It is assumed that the cellobiase enzyme (E_2) is not adsorbed on the insoluble cellulose (S).

The enzyme conservation equations for these reactions are:

$$E_0 = E + E^* + E^*S + E^*Cb + ECb + E^*G + EG \tag{8}$$

$$E_{20} = E_2 + E_2Cb + E_2G \tag{9}$$

Using the pseudo-steady-state assumption, the rate equations for the hydrolysis of cellulose into cellobiose ($-dS/dt = dCb/dt$) and of cellobiose into glucose (dG/dt) can be found:

$$-\frac{dS}{dt} = \frac{dCb}{dt} = \frac{V_{m2}S}{K_{m2}\left(\frac{1+K_{ad}}{K_{ad}}\right)\left(1+\frac{Cb-G}{K_{I2}}+\frac{G}{K_{I3}}\right)+S} \tag{10}$$

$$\frac{dG}{dt} = \frac{V_{m1}(Cb-G)}{K_{m1}\left(1+\frac{G}{K_{I1}}\right)+(Cb-G)} \tag{11}$$

where Cb is the total cellobiose formed; hence, the cellobiose present at any given time is $(Cb - G)$. For the inhibition of enzyme E [eqs. (3)–(4′)], the same affinity between inhibitor and enzyme has been assumed for the soluble (E) and adsorbed (E^*) fractions ($K_{I2} = K^*_{I2}$; $K_{I3} = K^*_{I3}$). For uniformity, the stoichiometric units have been normalized as mono-, di-, and polyanhydroglucose (this results in the molecular weights of glucose, cellobiose, and cellulose as 162, 324, and $n \times 162$). The term S is the substrate available for enzyme attack. The value $S = (\alpha S_0 - Cb)$ has been used, α being the fraction of initial substrate susceptible to attack by the enzymes.

Equation (11) has the form of a Michaelis–Menten equation with product inhibition. Equation (10) can also be expressed as such using apparent values for the Michaelis constant (K'_{m2}) and for the substrate concentration available (S'_0) [eq. (10′)]:

$$\frac{dCb}{dt} = \frac{V_{m2}(S'_0 - Cb)}{K'_{m2}\left(1 + \frac{Cb - G}{K_{I2}} + \frac{G}{K_{I3}}\right) + (S'_0 - Cb)} \qquad (10')$$

where

$$S'_0 = \alpha S_0 \quad \text{and} \quad K'_{m2} = K_{m2}\left(\frac{1 + K_{ad}}{K_{ad}}\right)$$

In a simplified mathematical form, the two equations can be expressed as:

$$\frac{dCb}{dt} = \frac{b_1(b_2 S_0 - Cb)}{1 + b_3 S_0 + b_4 Cb + b_5 G} \qquad (10'')$$

$$\frac{dG}{dt} = \frac{b'_1(Cb - G)}{1 + b'_2 Cb + b'_3 G} \qquad (11')$$

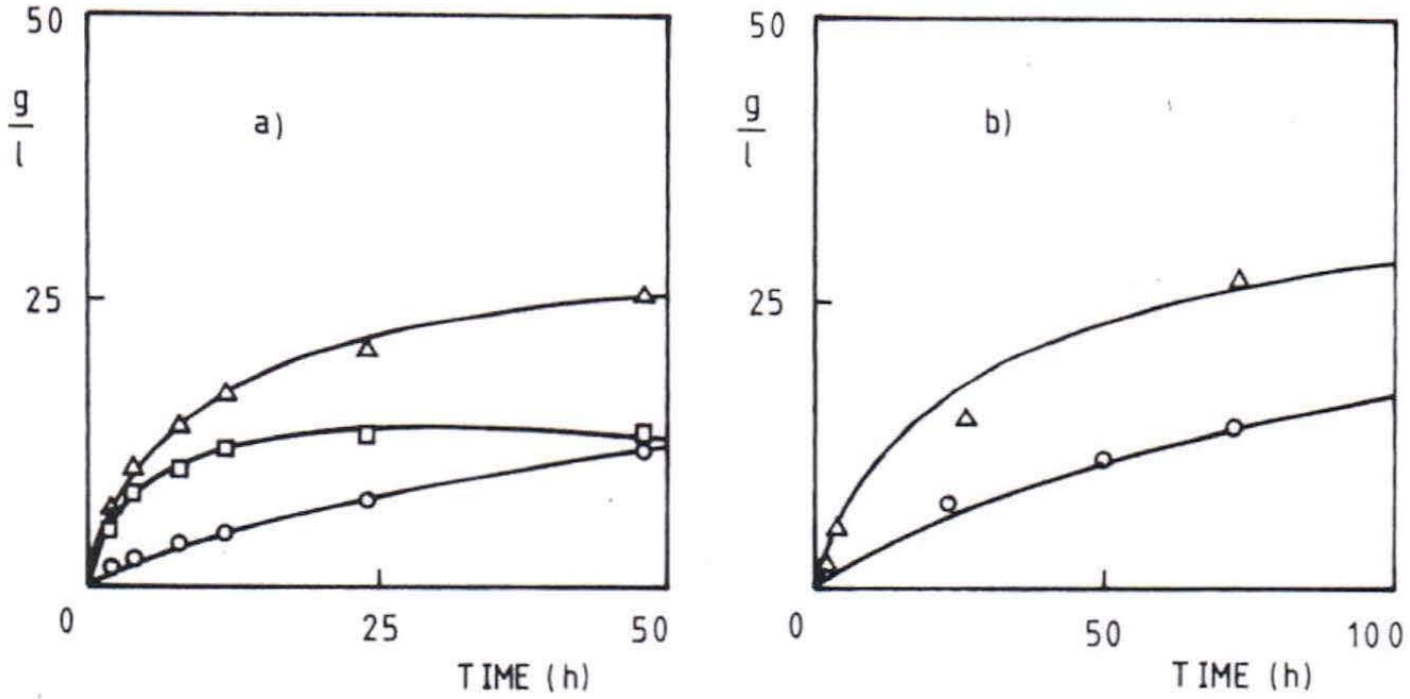

Fig. 1. Hydrolysis of Solka Floc. Comparison of experimental data with eqs. (10′), (11), and [(10′) − (11)]: (△) reducing sugars (total cellobiose formed), (○) glucose, and (□) cellobiose accumulated. Parameters are listed in Table I. The two sections show (a) Solka Floc SW40, using crude fungal cellulase from *Trichoderma* [Data from ref. 9 (temp = 50°C and pH 4.8)] and (b) Solka Floc BW300 using commercial cellulase (*Trichoderma*) supplemented with cellobiase [Data are from ref. 11 (temp = 35°C and pH 4.9)].

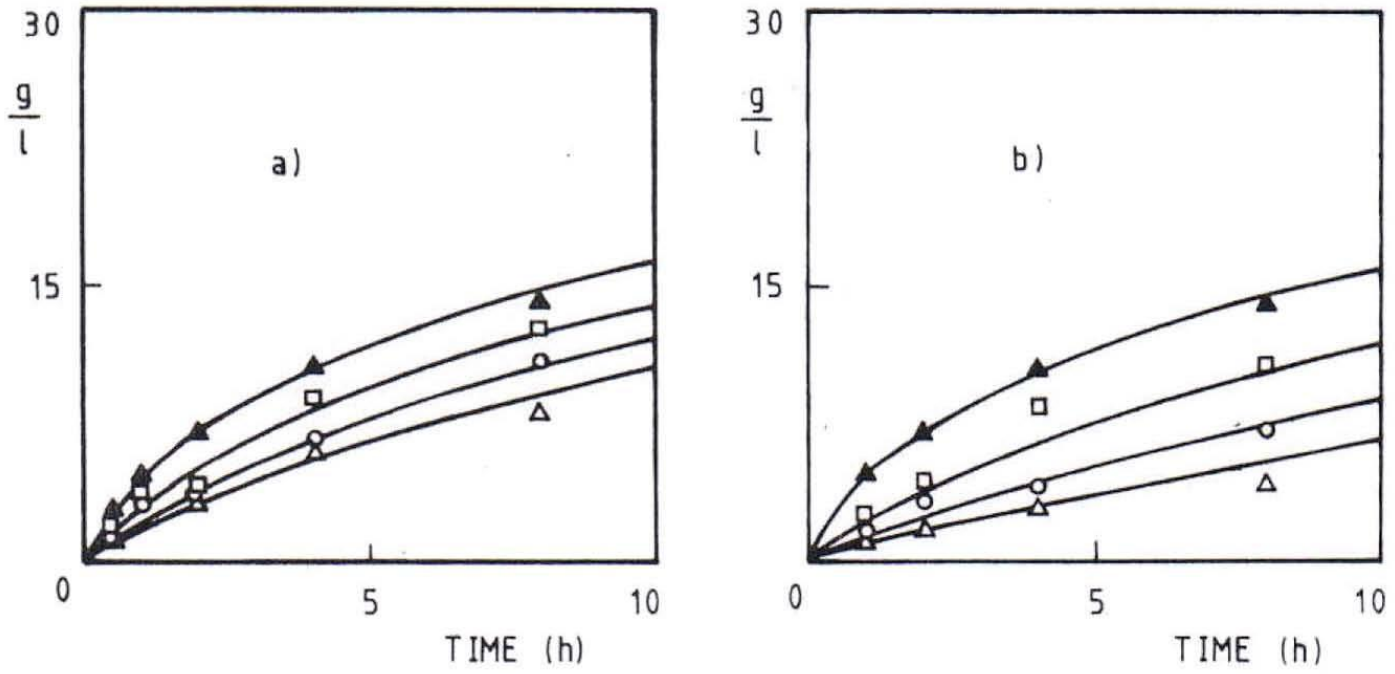

Fig. 2. Effect of glucose and cellobiose inhibition on the rate of cellulose hydrolysis. Data are from ref. 9. Solid lines correspond to eq. (10′). Inhibitor concentrations: (▲) 0 g/L, (□) 10 g/L, (○) 20 g/L, and (△) 30 g/L; for (a) glucose and (b) cellobiose.

TABLE I

Parameters Used in eqs. (10′) and (11)[a]

Parameter	Value	Comments
K'_{m2}	42.8	as determined by Howell and Mangat (ref. 10) for the hydrolysis of cellulose to cellobiose over 100 h using Solka Floc BW100 and a crude enzyme preparation from *Trichoderma* QM9123
K_{I2}	2.3	values determined using the experimental results of Lee (ref. 9) for glucose and cellobiose inhibition of cellulose hydrolysis (Fig. 2)
K_{I3}	6.1	
K_{m1}	0.86	as determined by Lee and Fan (ref. 4) for the hydrolysis of cellobiose to glucose using a crude enzyme preparation from *Trichoderma* QM9414
K_{I1}	0.1	
V_{m2}	18.0	values obtained for the hydrolysis of Solka Floc SW40 using a crude enzyme preparation from *Trichoderma* [Fig. 1(a)]
V_{m1}	1.31	
α	0.54	
V_{m2}	7.5	values obtained for the hydrolysis of Solka Floc BW300 using a commercial enzyme preparation from *Trichoderma* supplemented with cellobiase. The value of α was estimated as 0.65 according to Asenjo and Jew (ref. 12)
V_{m1}	1.3	
α	0.65	

[a]Units are g L^{-1} and g L^{-1} h^{-1}.

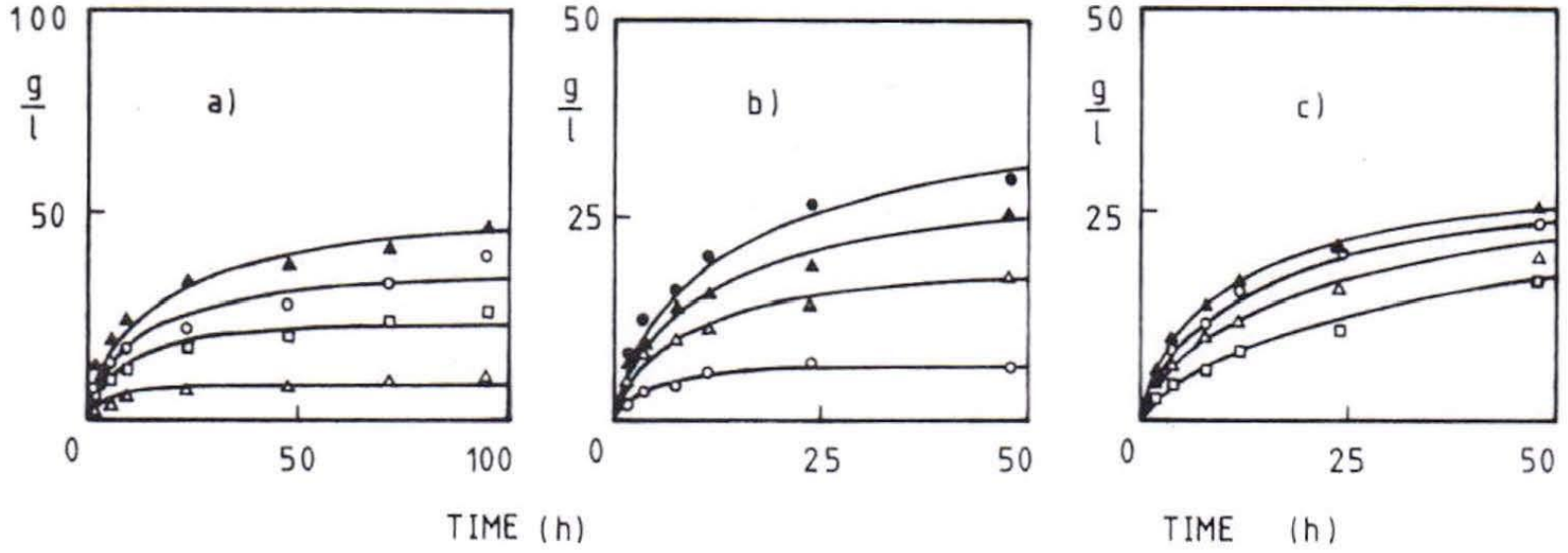

Fig. 3. Effect of substrate and of enzyme concentration in the hydrolysis of Solka Floc SW40. Experimental data are from ref. 9: (a) substrate pretreatment (ball milling) effect: (□) no pretreatment, (○) 24-h ball milling, (▲) 96 h, and (△) microcrystalline cellulose; (b) substrate concentration effect: (○) 10 g/L, (△) 30 g/L, (▲) 50 g/L, and (●) 75 g/L; (c) enzyme concentration effect: (▲) $E = 0.98$ g/L (normal concentration ($V_{m2} = 18$ and $V_{m1} = 1.31$); (○) $E = 0.71$ g/L ($V_{m2} = 13$ and $V_{m1} = 0.935$); (△) $E = 0.49$ g/L ($V_{m2} = 9.0$ and $V_{m1} = 0.66$); (□) $E = 0.25$ g/L ($V_{m2} = 4.6$ and $V_{m1} = 0.33$).

TABLE II

Effect of Mechanical Pretreatment of Substrate (Ball-Milling Time) on Value of α for Solka Floc SW40

Ball milling time (h)	α
0	0.48
24	0.71
96	0.98
Microcrystalline cellulose (no ball milling)	0.18

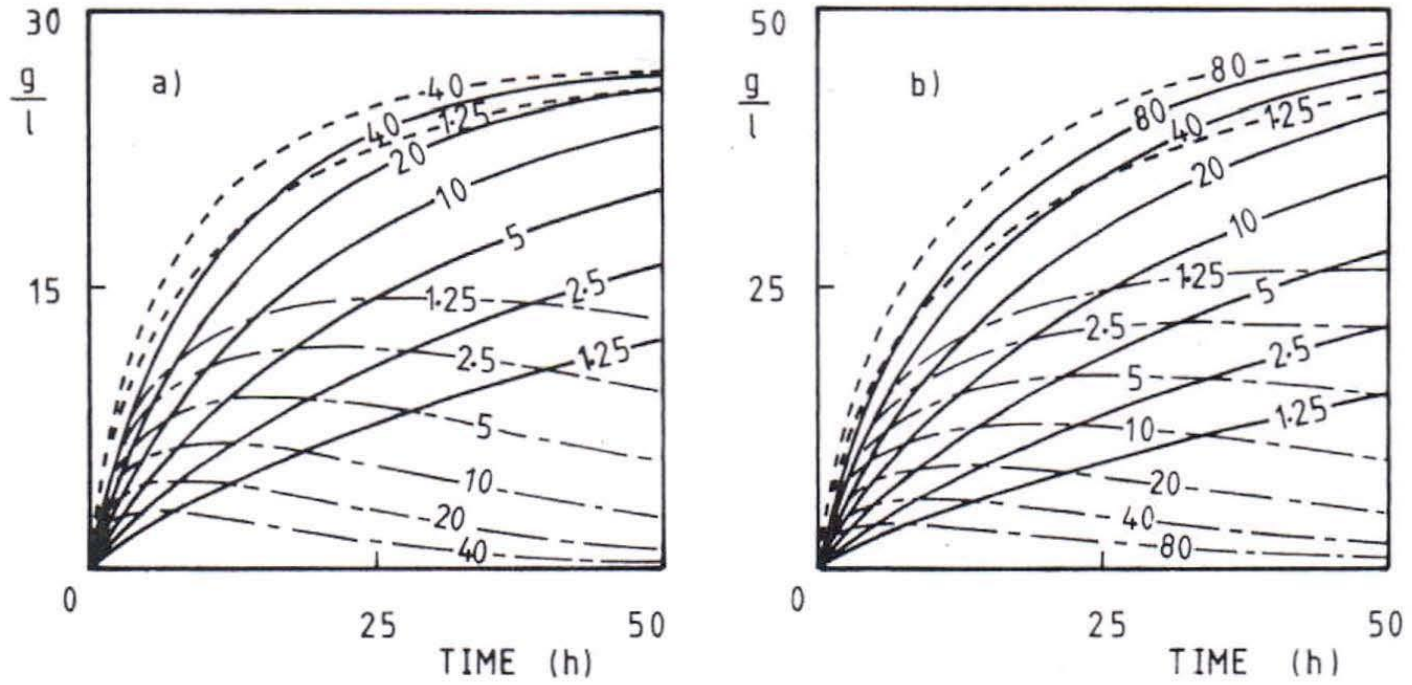

Fig. 4. Effect of increasing cellobiase activity in the hydrolysis of Solka Floc SW40 by a crude fungal cellulase preparation: (——) glucose, (-----) cellobiose, and (----) total cellulose hydrolyzed. Values are $V_{m2} = 20$ g/L h; $V_{m1} = 1.25$, 2.5, 5, 10, 20, 40, and 80 g/L h. Also, (a) $\alpha = 0.54$ (standard substrate; Table I) and (b) $\alpha = 0.98$ (96 h ball milled substrate; Table II).

BIOCHEMICAL ENGINEERING 111-413
Reprinted from
ANNALS OF THE NEW YORK ACADEMY OF SC (1982)

Primary Metabolite or Microbial Protein from Cellulose: Conditions, Kinetics, and Modeling of the Simultaneous Saccharification and Fermentation to Citric Acid

JUAN A. ASENJO AND CHUCK JEW

Biochemical Engineering Laboratory
Department of Chemical Engineering
and Applied Chemistry
Columbia University
New York, New York 10027

Scientific Notes

Process Kinetics and Bioreactor Design for the Direct Bioconversion of Cellulose into Microbial Products

JUAN A. ASENJO
Biochemical Engineering Laboratory,
Department of Chemical Engineering
and Applied Chemistry,
Columbia University,
New York, New York 10027

Biotechnology and Bioengineering Symp. No. 13, 449–456 (1983)

MODELLING THE BIOCONVERSION OF CELLULOSE INTO MICROBIAL PRODUCTS: RATE LIMITATIONS

By JUAN A. ASENJO

Biochemical Engineering Laboratory, Department of Chemical Engineering and Applied Chemistry, Columbia University, New York, New York 10027, USA.
Telephone: 280-2849/280-4453.

Process Biochemistry, December 1984
vol. 19

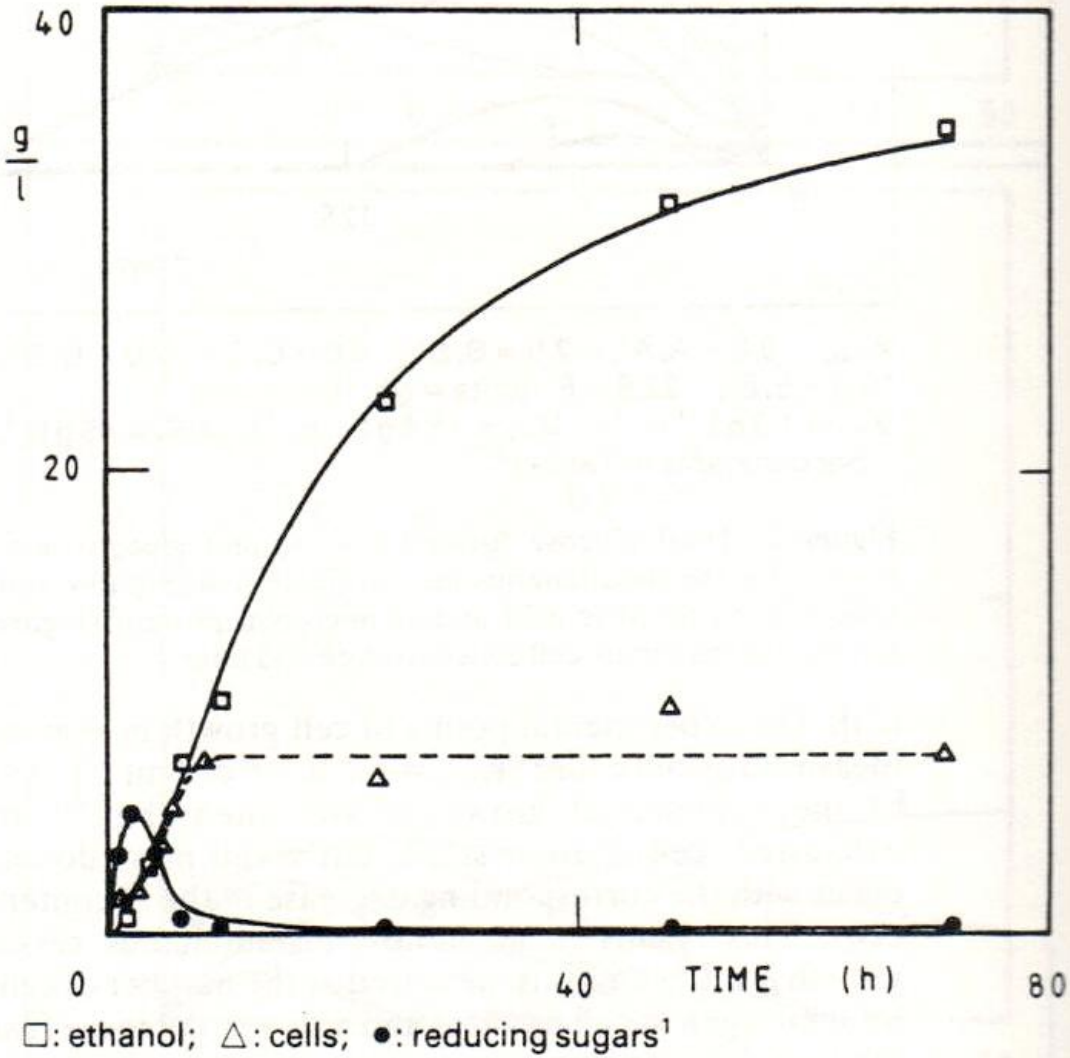

Figure 1: Experimental data and computer simulation of growth and production of ethanol in a direct simultaneous bioconversion (SSF) using *Saccharomyces carlsbergensis* IAM 4787 and *Trichoderma viride* cellulase. Substrate: 100 g l^{-1} cellulose powder (temperature = 40°C: pH = 5.0).

Optimization of Batch Processes Involving Simultaneous Enzymatic and Microbial Reactions

J. A. Asenjo
Biochemical Engineering Laboratory, University of Reading, Reading, England RG6 2AP

W.-H. Sun* and J. L. Spencer†
Department of Chemical Engineering and Applied Chemistry, Columbia University, New York, New York 10027

Received April 26, 1990/Accepted November 12, 1990

Biotechnology and Bioengineering, Vol. 37, Pp. 1087–1094 (1991)

Bioprocess Engineering 14 (1996) 323–329

Optimal control of batch processes involving simultaneous enzymatic and microbial reactions

J.A. Asenjo, W-H. Sun, J.L. Spencer

Received: 5 September 1995

J.A. Asenjo
Centre for Biochemical Engineering and Biotechnology,
Department of Chemical Engineering,
Universidad de Chile

W-H. Sun, J.L. Spencer
Department of Chemical Engineering, Materials Science and Mining Engineering, Columbia University, New York 10027, USA

Correspondence to: J.L. Spencer

The support of one of the authors by the National Science Foundation (Grant CBT-84-20552) is gratefully acknowledged.

ICDB

Institute for Cell Dynamics and Biotechnology: A Centre for Systems Biology

Institute for Cell Dynamics and Biotechnology: A Center for Systems Biology

Systems Biology

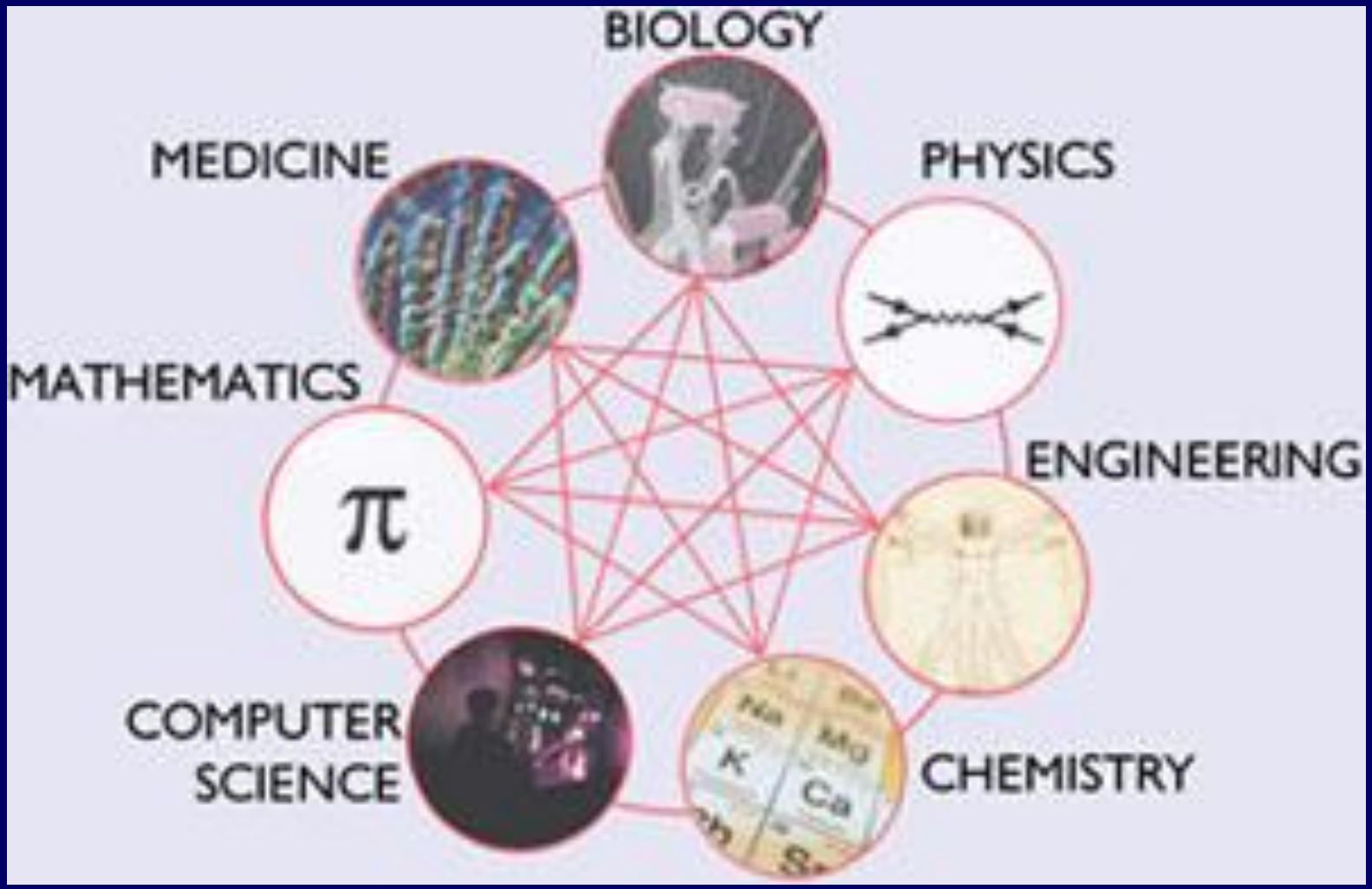

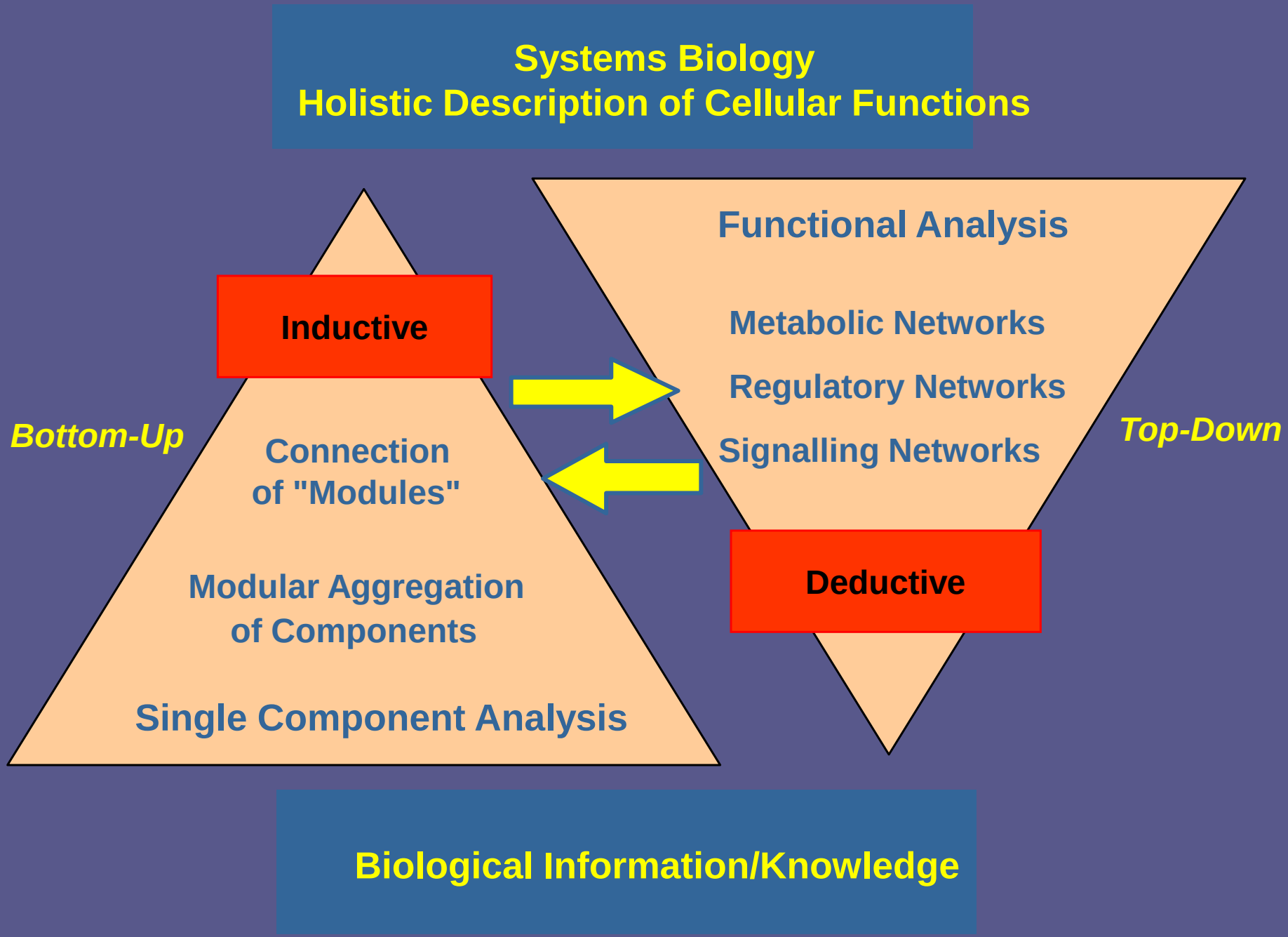
Systems Biology
Holistic Description of Cellular Functions
Functional Analysis
Metabolic Networks
Regulatory Networks
Signalling Networks
Inductive
Deductive
Bottom-Up
Top-Down
Connection
of "Modules"
Modular Aggregation
of Components
Single Component Analysis
Biological Information/Knowledge

ICDB

Institute for Cell Dynamics and Biotechnology: A Centre for Systems Biology

Second Workshop December 2008 at Marbella

We haven't the money, so we've got to think

Ernest Lord Rutherford, 1871 - 1937

ICDB

Institute for Cell Dynamics and Biotechnology: A Centre for Systems Biology

Metabolomics and Protein Engineering


ATLANTIC OCEAN
PRINCE EDWARD ISLANDS (S. Afr.)
SOUTH GEORGIA (UK)
SOUTH SANDWICH ISLANDS (UK)
CROZET IS. (Fr.)
SOUTHERN OCEAN
FALKLAND ISLANDS (UK)
South Orkney Is.
Scotia Sea
ARGENTINA
Weddell Sea
KERGUELEN (Fr.)
South Shetland Is.
Larsen Ice Shelf
Ronne Ice Shelf
HEARD & MCDONALD ISLANDS (Austr.)
CHILE
Antarctic Penin.
Alexander I.
Berkner I.
Amery Ice Shelf
ANTARCTICA
Vinson Massif 4897 m
South Pole
INDIAN OCEAN
Thurston I.
Mt. Kirkpatrick 4528 m
Ross Ice Shelf
Roosevelt I.
Ross Sea
SOUTHERN OCEAN
Balleny Is.
PACIFIC OCEAN
MACQUARIE I. (Austr.)
CAMPBELL IS. (N.Z.)
AUCKLAND IS. (N.Z.)
ANTIPODES IS. (N.Z.)
AUSTRALIA
NEW ZEALAND
40°
20°
0°
20°
40°
50°
60°
70°
80°
100°
120°
140°
160°
160°
140°

Random Mutagenesis (directed evolution)

Saturation Mutagenesis

Gene Shuffling

3-D Models (homology)

Site-Directed Mutagenesis

ICDB
Institute for Cell Dynamics and Biotechnology: A Centre for Systems Biology

Cold-Active Enzymes from Antarctica

1. **Trypsin**-like **Protease from Krill** – US Patent granted. **Medical applications**.

2. **Subtilisin-like Protease** from Pseudomonas sp. – US Patent filed. Use in **detergent industry.**

3. **Xylanase** from Psychrobacter sp. **-** US Patent filed. Use in **biofuels industry.**

ICDB
Institute for Cell Dynamics and Biotechnology: A Centre for Systems Biology

Increasing the Thermostability of a Xylanase using a Homology model

- Background
- **Psycrophilic xylanase**, complete sequence obtained, cloned and expressed in *E. coli* BL21(DE3)/pET22b(+).
- Active at **temperatures** between **5ºC-40ºC**, pH Optimum → 6 - 8
- Patent filed
- **Using directed evolution the Kcat was increased 3 times** but there was **no increase in thermostability**.
- Using a **homolgy model of structure** appropriate regions for **mutations** were found by **simulation of molecular dynamics** and **degree of compaction**.

ICDB
Institute for Cell Dynamics and Biotechnology: A Centre for Systems Biology

Results of simulation of molecular dynamics

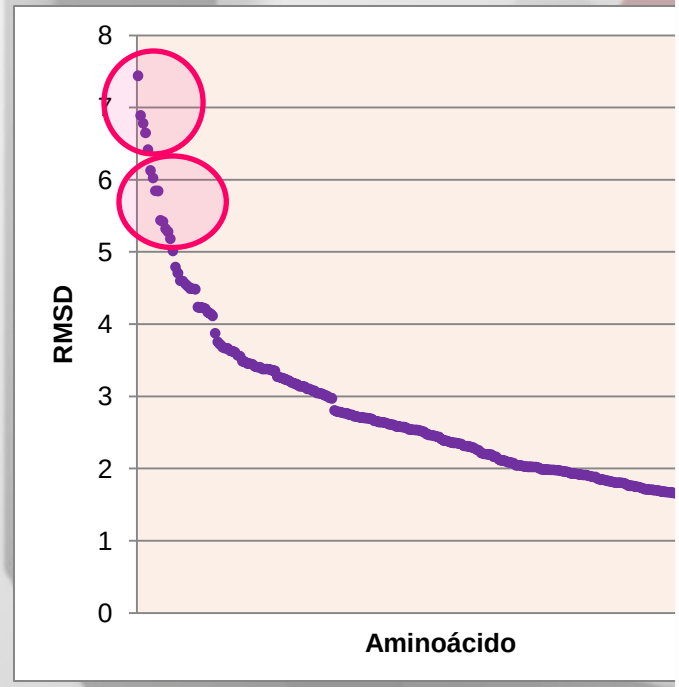

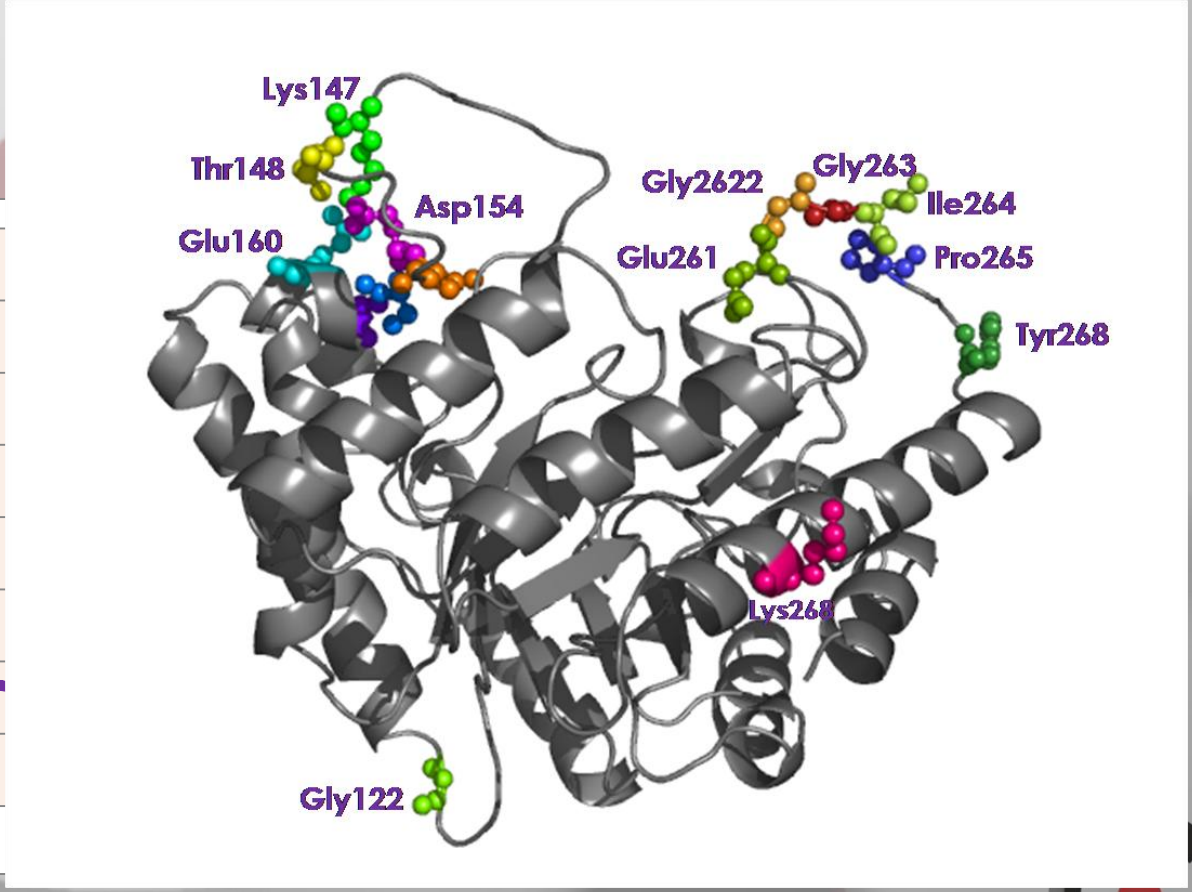

RMSD: a measure of how much each amino acid can move

ICDB
Institute for Cell Dynamics and Biotechnology: A Centre for Systems Biology

Selection of amino acids to mutate using a model of comparative compaction

- the program **compares** the **density of contact** between equivalent residues in 2 groups of enzymes.
- The density of contact is the **number of atoms** which can make contact with a residue.
- Distance < 4,5 Å
- Negative results indicate that the **compaction** in the cryophilic protein is **smaller** than in the mesophilic counterpart and these amino acids are therefore **targets for mutagenesis**.
- The **most promising target** was **SER221** as it is **near to the active site** and in a highly conserved region.

ICDB

Institute for Cell Dynamics and Biotechnology: A Centre for Systems Biology

GLN88	-2.01219512195
ALA308	1.42446043165
MET214	-1.31690140845
GLU285	-1.15833333333
VAL216	1.29559748428
SER222	-1.19117647059
GLY155	2.0
VAL249	-1.15853658537
ASN252	-1.41666666667
GLU127	-1.1393442623
THR41	-1.1640625
ALA289	1.20567375887
ALA229	1.44
ALA80	1.64485981308
SER345	3.05084745763
HIS84	-1.33695652174

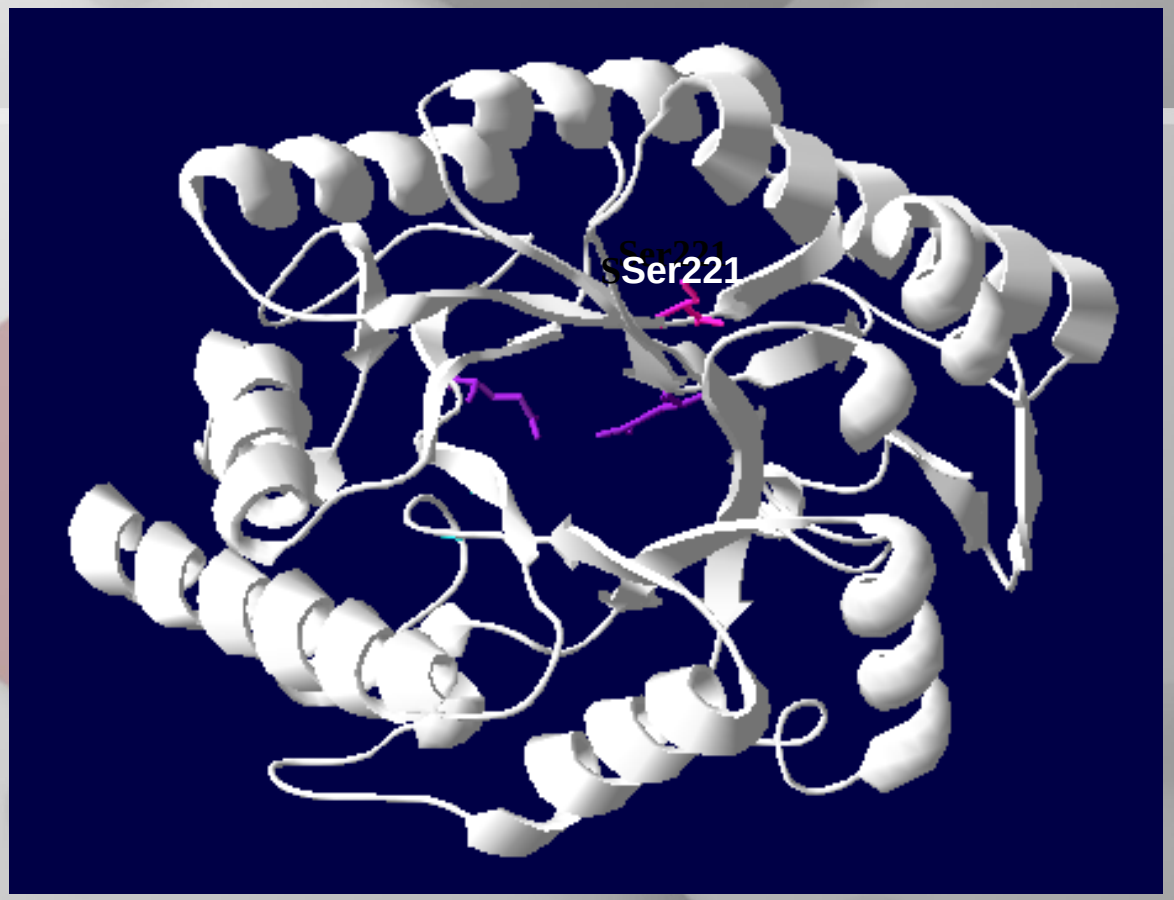


```
1CLX-H          DEAFRRARAADPTAELYYNDFNTEENGAKTTALVNLVQRLLNNGVPIDGVGFQMHVMNDY 220
1US3-H          ERAFQTARAADPAVILYYNDYNIEQNNAKTTKMVDMVKDFQARSIPIDGVGFQMHVCMNY 231
XIL-L-H         PLAYKAARAADPDADLYYNDYNLIWNADKLDAVIAMVNDFHNNGVPIDGIGFQSHISLNS 227
                  *:: ****** . *****:*   *  *   :: :*: :  ..:****:*** *:  :
```

ICDB

Institute for Cell Dynamics and Biotechnology: A Centre for Systems Biology

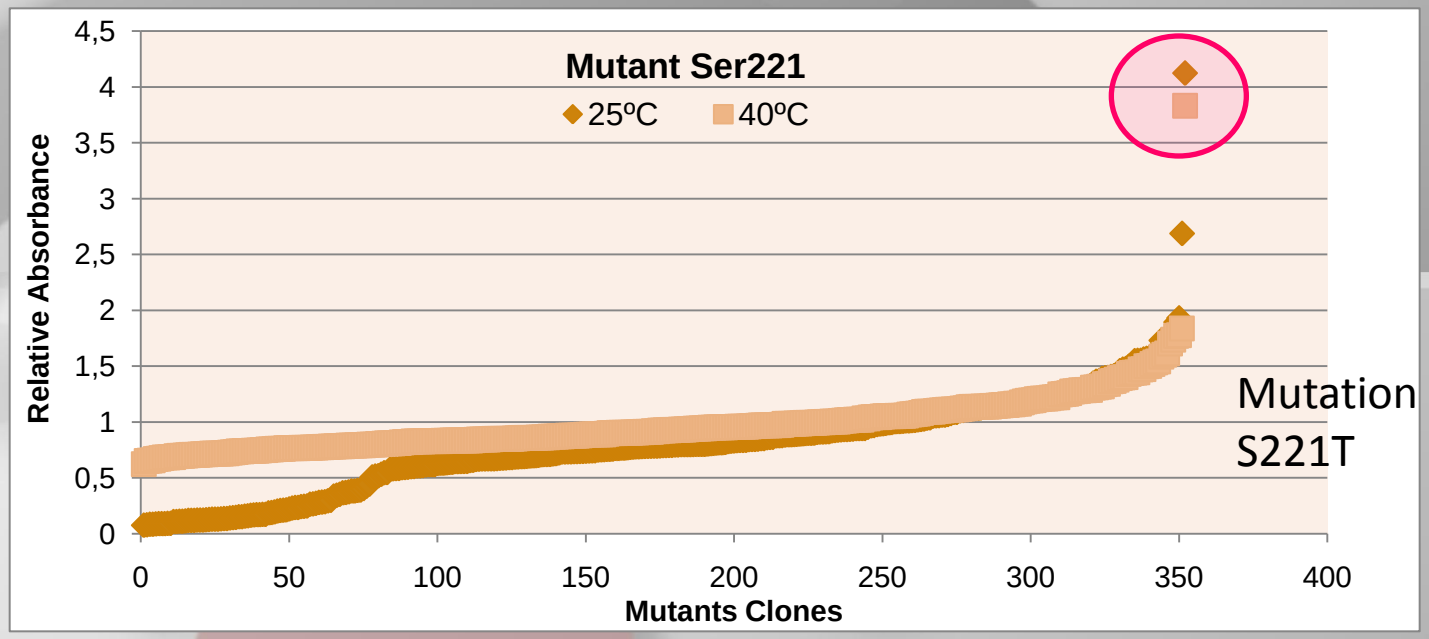

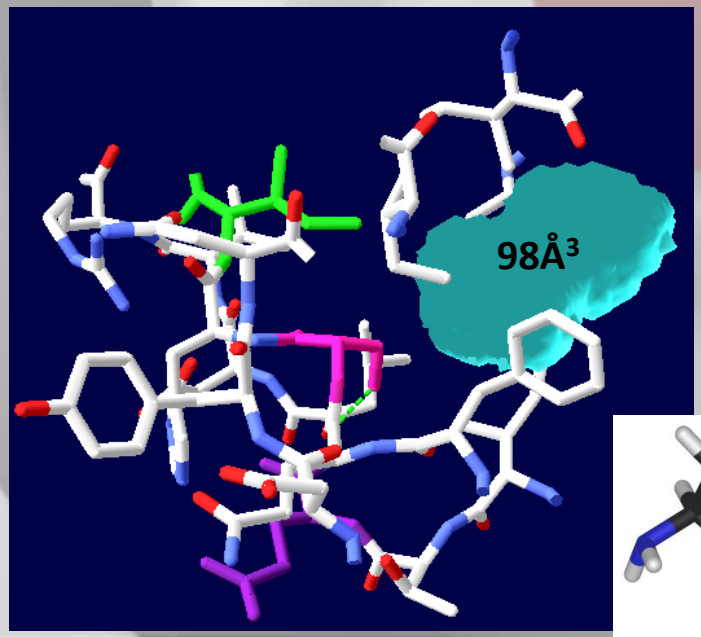

Cavity
Reduction

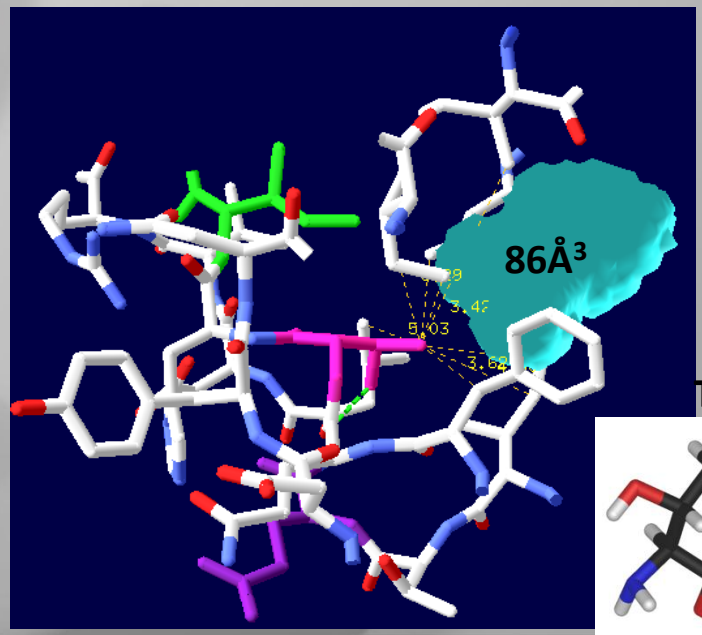

Ser

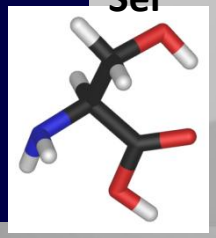

Thr

Improvement in the Thermostability of a Cold-Active Xylanase

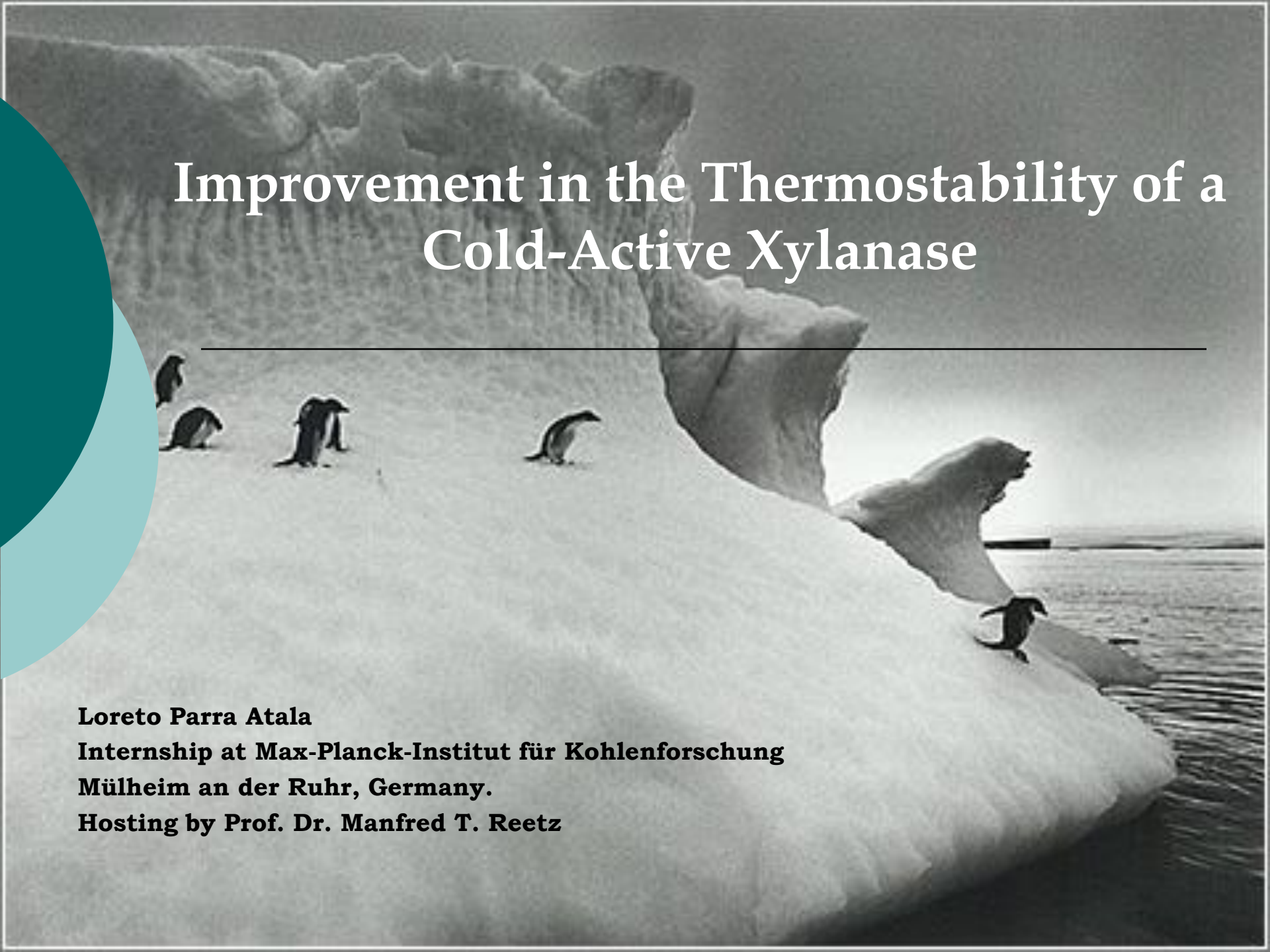

Loreto Parra Atala
Internship at Max-Planck-Institut für Kohlenforschung
Mülheim an der Ruhr, Germany.
Hosting by Prof. Dr. Manfred T. Reetz

Cold Active Enzymes Biotechnological Applications

High catalytic efficiency at low temperatures → reduction of the energy cost of a processes

- **Biotechnological Applications**
  - Additives in detergent; Cold washing (proteases, lipases, amylases and cellulases)
  - Additives in food industries
  - Environmental bioremediation
- **Problem → Thermolability**
  - The thermostability is necessary for the use of the enzyme in industrial processes
- **Solution → Protein Engineering**
  - Directed Evolution (Random Gene Mutagenesis) epPCR and DNA Shuffling
  - Rational Design (3D protein structure) Point mutations (saturation mutagenesis)

Library C + Focused epPCR B

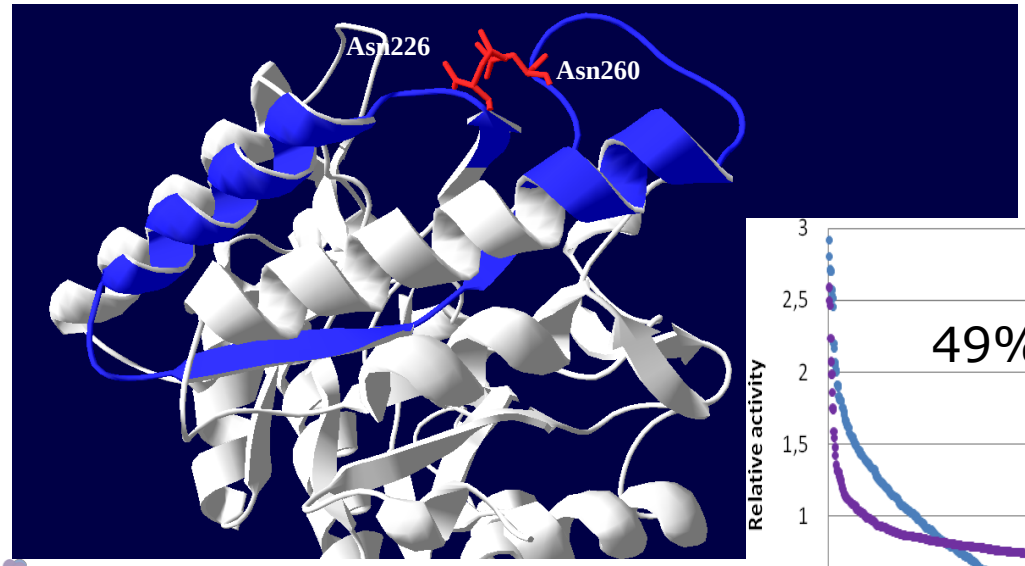

Was designed in order to anchor a flexible loop to a rigid part of the protein.

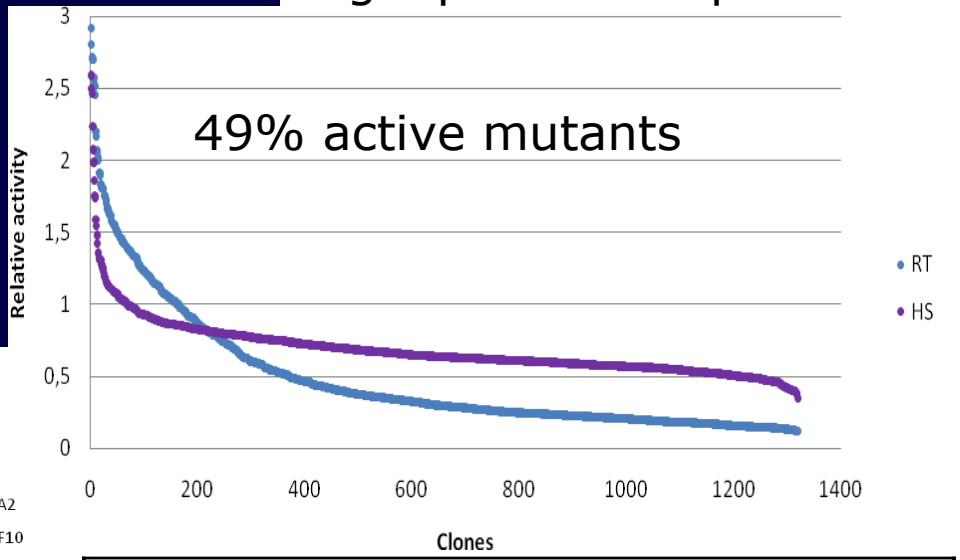

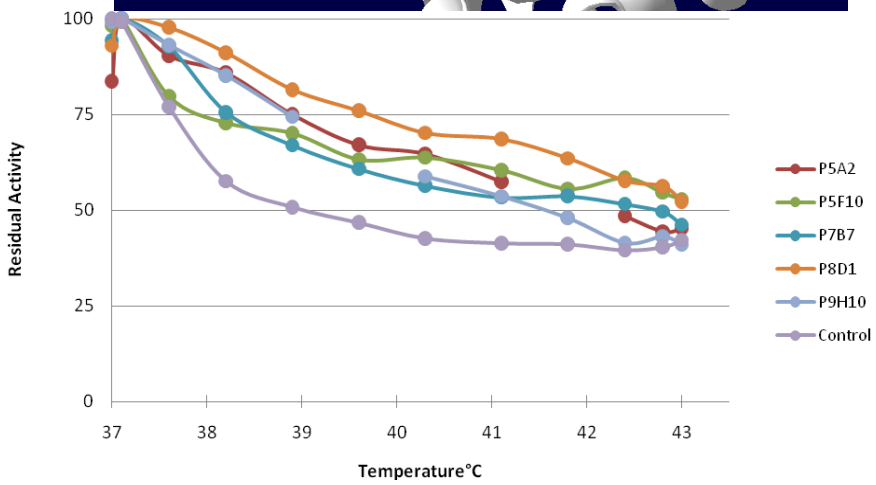

Clone	$\Delta T_{50}{}^{15}$ °C	Mutations
P5F10	4.3	Val249Ile
P8D1	4.1	Asn226Leu/Gly262Ser/Ile264Ser
P7B7	3.8	Asn226His
P5A2	3.2	Asn260Ser
P9H10	2.5	Asn226Pro

ICDB

Institute for Cell Dynamics and Biotechnology: A Centre for Systems Biology

Metabolomics

ICDB
Institute for Cell Dynamics and Biotechnology: A Centre for Systems Biology

Metabolomics of Recombinant Yeast

- Metabolic Flux Analysis
- Microarrays of Gene Expression
- Integration of Gene Expression and Regulation with Metabolic Fluxes
- Modelling Metabolic Fluxes and Gene Regulation

Metabolomics

Metabolic Flux Analysis

Gonzalez, R., Andrews, B.A. Molitor, J. and Asenjo, J.A. (2003) *Biotechnol. Bioeng.*, 82, 152-169.

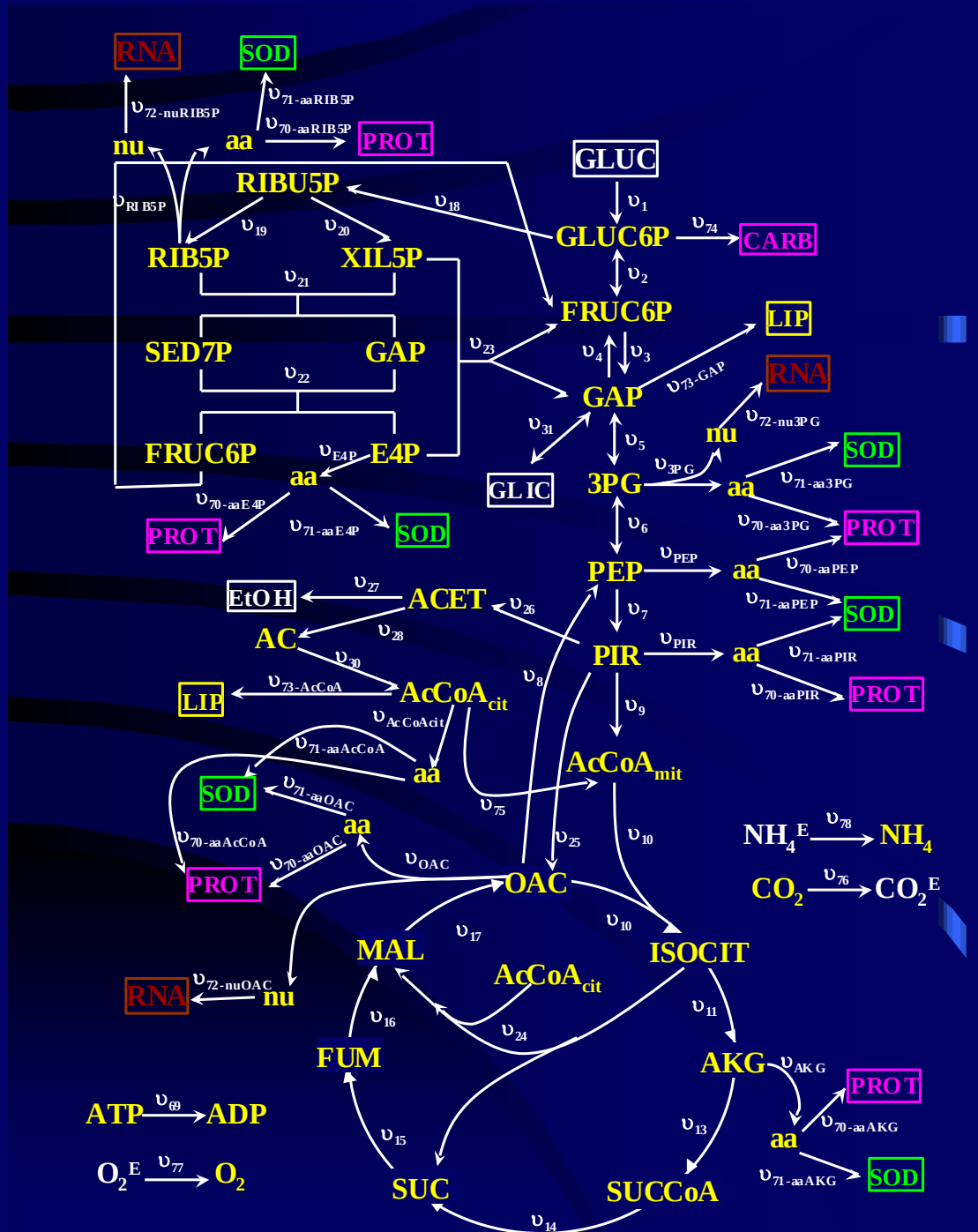

Metabolic Flux Analysis

Metabolic Flux Balance

$$dX/dt = S\,v - b$$

in SS: $S\,v = b$ or $S\,r = 0 \rightarrow S_c\,r_c + S_m\,r_m = 0$

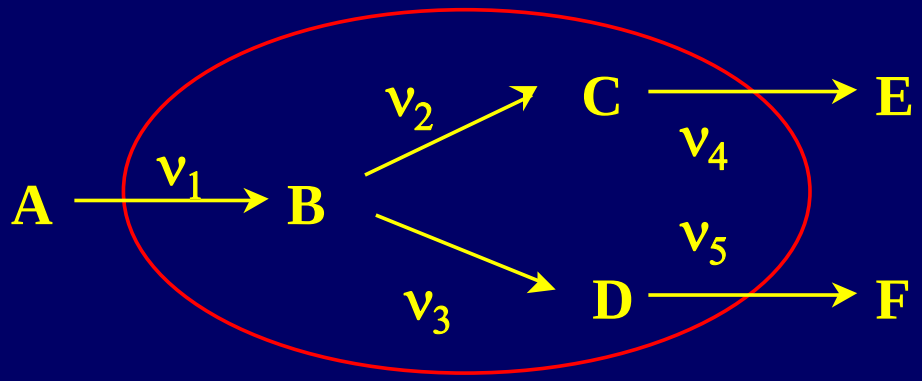

S	Stoichiometric Matrix
r	Rate (Flux) vector
c	Calculated
m	Measured

$S\,r=0=$

	ν_1	ν_2	ν_3	ν_4	ν_5
B	1	-1	-1	0	0
C	0	1	0	-1	0
D	0	0	1	0	-1

ν_1 ν_2 ν_3 ν_4 ν_5

⇒

	ν_1	ν_2	ν_3
B	1	-1	-1
C	0	1	0
D	0	0	1

ν_1 ν_2 ν_3

+

	ν_4	ν_5
B	0	0
C	-1	0
D	0	-1

ν_4 ν_5

RATIO P-/P+ GLUC